Front. Chem. Sci. Eng. 2022, 16(5): 709–719
https://doi.org/10.1007/s11705-021-2078-2

RESEARCH ARTICLE

Fabrication of high-performance pervaporation composite membrane for alkaline wastewater reclamation

Guiqin Bai[1], Jianzhong Xia (✉)[2], Bing Cao[1], Rui Zhang[1], Junquan Meng[1], Pei Li (✉)[1]

1 College of Materials Science and Engineering, Beijing University of Chemical Technology, Beijing 100029, China
2 Institute for Advance Study, Shenzhen University, Shenzhen 518060, China

Abstract Pervaporation desalination has a unique advantage to recycle concentrated salt solutions. The merit can be applied to treat alkaline wastewater if the membrane has superior alkali-resistance. In this paper, we used polyethylene microfiltration membrane as the substrate and deposited a glutaraldehyde crosslinked sodium carboxymethylcellulose layer by spray-coating. Pervaporation flux of the composite membrane reached 35 ± 2 kg·m^{-2}·h^{-1} with a sodium chloride rejection of $99.9\% \pm 0.1\%$ when separating a 3.5 wt-% sodium chloride solution at 70 °C. The desalination performance was stable after soaking the membrane in a 20 wt-% NaOH solution at room temperature for 9 d and in a 10 wt-% NaOH solution at 60 °C for 80 h. Moreover, the membrane was stable in 4 wt-% sulfuric acid and a 500 mg·L^{-1} sodium hypochlorite solution. In a process of concentrating a NaOH solution from 5 to 10 wt-% at 60 °C, an average water flux of 23 kg·m^{-2}·h^{-1} with a NaOH rejection over 99.98% was obtained.

Keywords pervaporation, alkaline solution concentration, polyethylene membrane, acid resistance, chlorine tolerance

1 Introduction

Alkaline wastewater is a common effluent in textile industry that uses cellulose as the major raw material [1–3]. To tune the hydrophilicity, surface morphology, tensile strength of cellulose, or enhance luster and the absorption rate of dye in dyeing and finishing engineering, cellulose is often soaked in a NaOH solution to destroy its crystalline structure [4]. However, this inevitably generates a large amount of alkaline wastewater. Common methods to treat alkaline wastewater are neutralization, electrodialysis and diffusion dialysis. Neutralization is simple but costly. Besides, a large amount of salt will be produced and discharged. Electrodialysis [5] demands a high capital investment, while diffusion dialysis needs high technical support with low recovery rate [6].

Membrane separation has merits of simple operation, energy-saving and environmental benign [7–10]. Reverse osmosis and nanofiltration have been applied to recycle water from NaOH wastewaters. However, at high alkali concentrations, the two pressure-driven processes need to overcome a very high osmotic pressure [11,12]. This limits their feasibility for industrialization. On the other hand, pervaporation membrane can be operated under atmospheric pressure and it has also been studied in biofuel dehydration in recent years [13]. In addition to that the driving-force of pervaporation is not sensitive to the ion concentration. Thus, pervaporation have been studied for desalinating concentrated brine solutions [14–18].

The key to treat concentrated alkaline solutions is to utilize a membrane material having sufficiently high alkaline resistance. Sodium carboxymethylcellulose (CMC-Na) has excellent resistance to alkali [19]. CMC-Na is formed in two steps. First, cellulose is reacted with NaOH to form alkaline cellulose; and second, the alkaline cellulose is etherified with monochloroacetic acid [20]. CMC-Na has a large number of hydroxyl and carboxylic groups. The ring structure of CMC-Na increases the polymer's free volume and the $-COO^-$ groups are hydrophilic. Moreover, CMC-Na is biodegradable, nontoxic, harmless and low cost. Therefore, CMC-Na is an ideal material for making alkali-resistant water permeable membranes.

Prasad et al. [21] crosslinked a polymer blend of CMC-Na/polyvinyl alcohol by glutaraldehyde (GA) and used it as the selective layer of composite pervaporation mem-

Received February 21, 2021; accepted June 1, 2021

E-mails: xiajianzhong@outlook.com (Xia J),
lipei@mail.buct.edu.cn (Li P)

branes. These membranes showed good performance for isopropanol dehydration. Zhang [22] and Gao [23] prepared a series of CMC-Na/polyvinyl alcohol-polysulfone (PVPS) composite nanofiltration membranes that exhibited good acid, alkaline and chlorine resistances. Although the selective layer material showed good alkali resistance, the commonly used substrates such as polyvinylidene fluoride (PVF), polyether sulfone (PES) and PVPS only have limited alkaline resistance. PVF decomposes in concentrated alkali solutions and loses mechanical strength [24,25]. The allowable pH range of PVPS and PES is 1–13 [26]. Compare with the above three polymers, polyolefins have much stronger chemical stability. For example, polyethylene (PE) has good mechanical properties, easy to process, good chemical stability, excellent acid and alkali resistance [27]. However, PE has poor adhesion to other materials due to the low surface energy. To our best knowledge, very few studies used PE as the substrate to prepare composite membranes [28–32]. Although the hydrophilicity of PE can be improved by plasma treatment [33], surface grafting [34] or ultraviolet irradiation [35], these methods are costly and complicated.

In previous reports, we demonstrated that spray-coating can improve the compatibility between hydrophobic and hydrophilic materials [36,37]. Here in this study, we spray-coated the CMC-Na polymer on top of a PE microfiltration membrane. The CMC-Na layer was further crosslinked by GA. The resulting CMC-Na/GA-PE composite membrane showed a stable pervaporation performance in 10–20 wt-% NaOH, 4 wt-% H_2SO_4 and 500 mg·L^{-1} NaClO solutions.

2 Experimental

2.1 Materials

Flat-sheet PE microfiltration membrane was provided by Beijing Origin Water Technology Co., Ltd. (China). CMC-Na (degree of substitution = 0.7, Mw = 250000 g·mol^{-1}) was purchased from RON Chemical Reagent Company (China). GA aqueous solution (50 wt-%), NaCl (purity ⩾ 99.5%), and NaOH (purity ⩾ 96%) were obtained from Tianjin Fuchen Chemical Reagent Factory (China). Concentrated H_2SO_4 (98%) was bought from Tianjin Damo Chemical Reagent Factory (China). Humic acid (HA, purity ⩾ 90%) was purchased from Shanghai Maclin Biochemical Co., Ltd. (China). Sodium alginate was bought from Sinopharm Chemical Reagent Co., Ltd. Deionized water was obtained from a laboratory-equipped RO water system. All chemicals were analytical grade and used without further purification.

2.2 Preparation of the CMC-Na/GA-PE composite membranes

The CMC-Na polymer was dissolved in deionized water to form a 2 wt-% CMC-Na solution. Initially, 3 g of 50 wt-% GA aqueous solution, 1 g 98 wt-% H_2SO_4 and 96 g deionized water were mixed together to prepare the crosslinking solution. GA and H_2SO_4 were used as the crosslinker and catalyst, respectively. To prepare the CMC-Na coating solutions, 6 g of the 2 wt-% CMC-Na solution was mixed with the crosslinking solution of 3, 4, 5, 6, and 8 g, respectively. This was to optimize the composition of the coating solution. The solution mixture was stirred at room temperature for 2 h before use. Figure 1 shows the procedure of making the composite membranes. Specifically, a piece of PE membrane was rinsed by ethanol and stuck on a glass board. Then, 1 mL of coating solution was sprayed on the PE membrane by an airbrush with a nozzle diameter of 0.3 mm. The airbrush was operated at a pressure of 0.3 MPa. After coating, the membrane was crosslinked at 100 °C for 2 to 5 h to obtain the CMC-Na/GA-PE composite membrane.

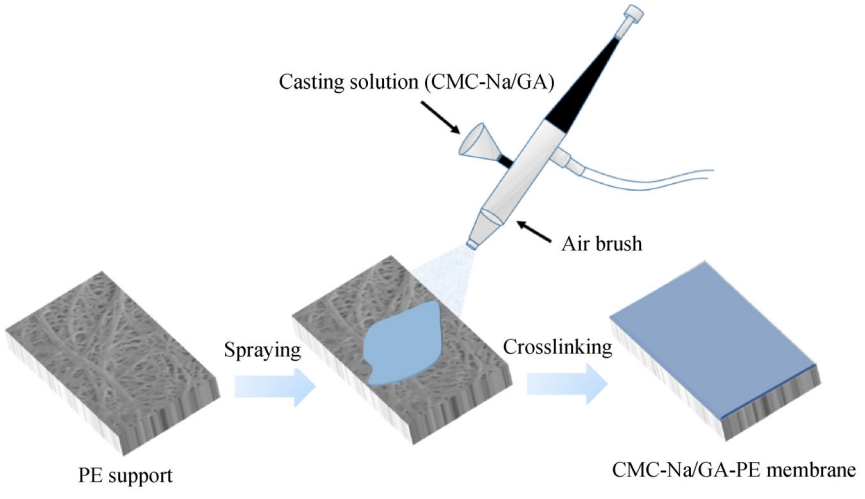

Fig. 1 A schematic diagram showing the method of preparing the CMC-Na/GA-PE composite membrane.

2.3 Characterization of the composite membranes

FTIR spectra of the composite membranes were recorded using a PerkinElmer 782 Fourier transform spectrophotometer. Range of the wavelength was from 4000 to 500 cm^{-1}. Elemental composition of the surfaces of the composite membranes was determined by energy dispersive spectroscopy (EDS, HITACHI S-4700).

Crystallinity of the pure CMC-Na and GA crosslinked CMC-Na were determined at room temperature using an ultima IV goniometer equipped with Cu-Kα monochromatic radiation (40 kV, 40 mA). Polymeric films were dried and placed on a quartz plate and scanned at a range of 5°–90° with a step of 0.02°. To investigate the change of crystallinity before and after alkali-soaking, X-ray diffraction (XRD) of self-supported membrane before and after NaOH-soaking was tested, respectively.

Morphologies of the composite membranes were observed by scanning electron microscope (SEM, HITACHI S-7800 Japan). To obtain a smooth cross-sectional morphology, the sample was wetted with ethanol and fractured in liquid nitrogen. The thicknesses of the composite membranes were measured based on their SEM images using the Nano Measurer 1.2 software. Before carrying out SEM tests, all samples were sputter-coated with gold.

2.3.1 Determining the swelling and crosslinking degrees of the free-standing CMC-Na/GA crosslinked polymers

The CMC-Na/GA coating solution was poured in a glass dish. After evaporated for 48 h, a film formed and then crosslinked for 4 h at 100 °C in a muffle furnace. The crosslinked CMC-Na/GA film was rinsed with deionized water for three times to remove the unreacted substance.

To measure swelling degree, the crosslinked CMC-Na/GA film was dried at room temperature for 24 h and weighed to obtain M_0. After that, the film was soaked in deionized water for 36 h to reach sorption equilibrium. The wet film was taken out, wiped with tissue and weighted to obtain M_1. The swelling degree was calculated by Eq. (1):

$$S = \frac{M_1 - M_0}{M_0} \times 100\%. \tag{1}$$

An average value resulting of three independent experiments were reported. The cross-linking degree was calculated by using following formula [38] Eq. (2):

$$\frac{\overline{M_c} = -\rho \overline{V_1} {\varphi_2}^{1/3}}{\ln\varphi_1 + \varphi_2 + \chi {\varphi_2}^2}, \tag{2}$$

where φ_1 was the solvent volume fraction, φ_2 was the volume fraction of the polymer, χ was the Flory-Huggins interaction parameter between solvent and polymer, $\overline{V}_1$ was the solvent molar volume, ρ was the polymer density, and $\overline{M_c}$ was the average molecular weight between two adjacent crosslinking points. ρ was measured using the Archimedes buoyance method [39], using Eq. (3):

$$\tilde{n} = \frac{A}{A-B}(\rho_0 - \rho_L) + \rho_L, \tag{3}$$

where A was the mass of the membrane in air, B was the mass of the membrane in an auxiliary liquid, ρ_L was the density of the auxiliary liquid, and ρ_0 was the density of air. χ was calculated by Eq. (4) [40]:

$$\chi = -\frac{\ln(1-\varphi_i) + \varphi_i}{{\varphi_i}^2}, \tag{4}$$

where φ_i was the volume fraction of the water-swelled polymer film.

2.3.2 Water contact angle and pervaporation tests of the composite membranes

To measure the water contact angle, a membrane sample was dried in vacuum and cut into a rectangular sheet with a dimension of 2 cm × 2 cm. An angle goniometer (DSA 100, KRUSS, Germany) was used to determine the water contact angle by dropping a water droplet of 3 μL onto the sample. Each sample was measured five times and the average value was reported.

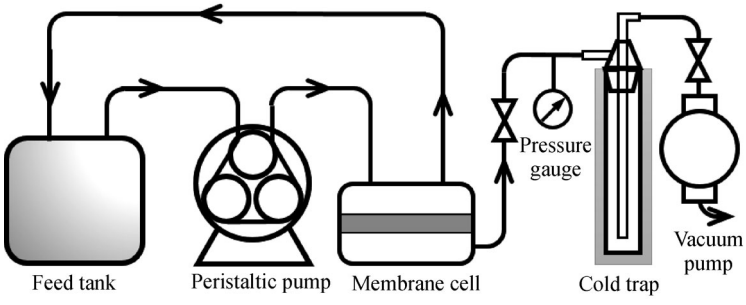

Fig. 2 The equipment set-up of the pervaporation test.

Pervaporation tests were carried out using a bespoke pervaporation equipment as shown in Fig. 2. A 3.5 wt-% NaCl solution was circulated at a flow rate of 0.1 $m \cdot s^{-1}$ at 70 °C while the pressure of the membrane permeate side was 100 Pa. The effective area of the composite membrane was 3.8 cm^2. Water vapor coming out from permeate side was collected by a liquid nitrogen cold trap.

The pervaporation flux (J) was calculated using Eq. (5). To calculate salt or NaOH rejection, the permeate solution was used to wash the membrane back side to dissolve the precipitated salt or NaOH.

$$J = \frac{M_1}{A_1 t_1}, \tag{5}$$

where M_1 was weight (kg) of the permeate, A_1 represented effective area (m^2) of the composite membrane, and t_1 was operation time (h). The salt or NaOH concentrations on the feed solution and permeate solution were measured by a conductivity meter (Oakton Con 110). Rejection R was calculated using Eq. (6):

$$R = \left(1 - \frac{C_p}{C_f}\right) \times 100\%, \tag{6}$$

where C_f and C_p were NaOH concentrations of feed and permeate, respectively.

2.3.3 Evaluation of the chemical resistances of the composite membranes

The dynamic and static alkaline resistance experiments were carried out for the composite membranes. To perform the static tests, the composite membranes were soaked either in a 20 wt-% NaOH solution for 9 d at 25 °C or in a 10 wt-% NaOH solution for 80 h at 60 °C. After soaking, the membrane was washed by deionized water before test. Pervaporation desalination properties of the membranes before and after the static soaking tests were compared to evaluate the membranes' stability in alkaline solution. For the dynamic tests, the composite membranes were used to extract water from a 10 wt-% NaOH solution at 60 °C in a 36 h pervaporation test where the feed flow rate was kept at 0.4 $m \cdot s^{-1}$. At last, a composite membrane was used to concentrate a NaOH solution from 5 to 10 wt-% in a pervaporation test to evaluate its ability to enrich alkaline solution.

To determine the acid resistance, a composite membrane was immersed in a 4 wt-% H_2SO_4 solution for 9 d. Water fluxes and salt rejections before and after the acid treatment were compared to evaluate the acid resistance.

To evaluate the chlorine resistance, a composite membrane was soaked in a 500 $mg \cdot L^{-1}$ sodium hypochlorite aqueous solution at 25 °C for 9 d. The pervaporation desalination properties were compared before and after the soaking test.

2.3.4 Thermal stability, mechanical performance, and fouling tests

The thermal stabilities of the CMC-Na/GA films before and after NaOH immersion were measured by thermogravimetric analysis (TGA, HTG-1). It was operated from 25 °C to 600 °C at a heating rate of 10 $°C \cdot min^{-1}$.

The mechanical properties of CMC-Na/GA films before and after NaOH immersion were measured by dynamic thermomechanical analysis (DMA, Q800 TA Instruments, USA). The sample was made into a strip of 15 mm long and 5 mm wide. The sample was mounted between two clamps and being stretched at a constant rate of 0.2 $N \cdot min^{-1}$ until it was broken. The program automatically recorded the tensile and deformation data to generate the stress-strain curves.

To evaluate the fouling behaviors of the CMC-Na/GA-PE composite membranes, a solution having 5000 $mg \cdot L^{-1}$ sodium alginate (SA) or HA was used as feed. The pervaporation tests were performed at 70 °C. Changes in membrane fluxes were monitored over time for 24 h. Deionized water was added to the feed solution every hour to maintain a constant feed concentration.

3 Results and discussion

3.1 Determination of the chemical structures of the composite membranes

Figure 3 exhibits the chemical structures of the composite membranes. A broad absorption band at 3250–3435 cm^{-1} is ascribed to the stretching vibration of –OH groups of CMC-Na chains in Fig. 3(a) [30]. While for the GA crosslinked CMC-Na polymer, the peak becomes smaller due to that part of the –OH groups have reacted with the –CHO groups of the GA. In addition, the peak at 1043 cm^{-1} representing the stretching vibration of C–O–C bonds [41] is stronger that indicating the formation of the crosslinking bonds. According to Fig. 3(b), the GA crosslinked CMC-Na shows a weaker and broader peak at 22.8° compared with that of the pristine CMC-Na polymer. This peak represents the crystalline regions of CMC-Na [42]. The relatively low and wide peak is the result of crosslinking that restricts the mobility of the CMC-Na polymer chains and limits chain packing for forming crystalline structure. All results prove that the cross-linking reaction between CMC-Na and GA occurs as shown in Fig. 3(c).

3.2 SEM images of the PE and CMC-Na/GA-PE composite membranes

Figure 4 shows the SEM images of the PE and CMC-Na/GA-PE composite membranes. The PE membrane has a typical melt-stretch structure with a thickness of 20 μm as shown in Fig. 4(a). A CMC-Na/GA dense layer with a

thickness of 2.2 ± 0.3 μm is formed on top of the PE membrane according to Figs. 4(b) and 4(c). The rough surface is caused by the accumulation of liquid droplets during the spray-coating process.

3.3 Optimizing the fabrication parameters of the CMC-Na/GA-PE composite membranes

The relations between the desalination properties and the fabrication parameters of the CMC-Na/GA-PE composite

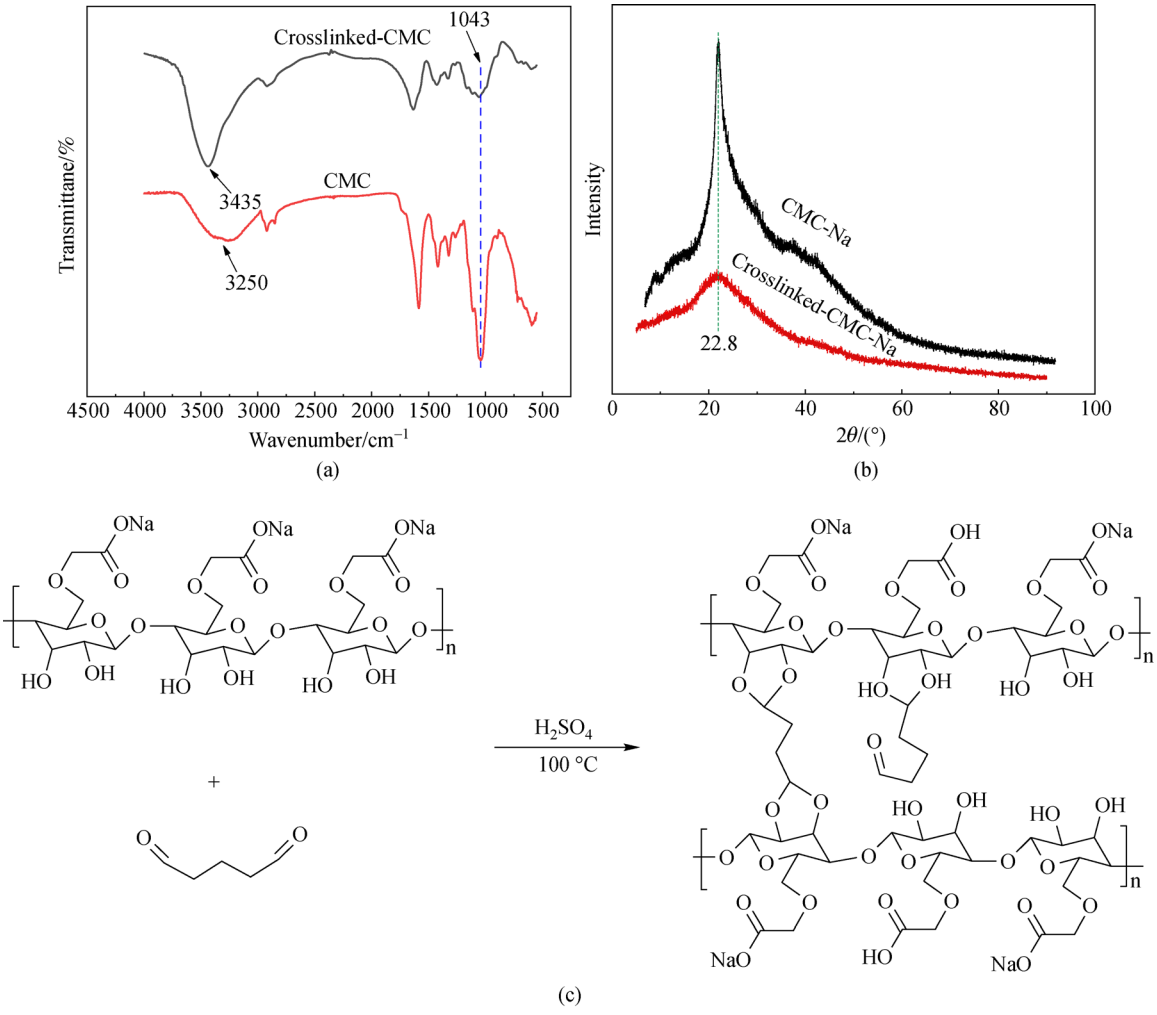

Fig. 3 (a) The FTIR spectra of the CMC-Na and crosslinked-CMC-Na; (b) the XRD patterns of CMC-Na and crosslinked-CMC-Na; (c) the schematic diagram for crosslinking CMC-Na using GA.

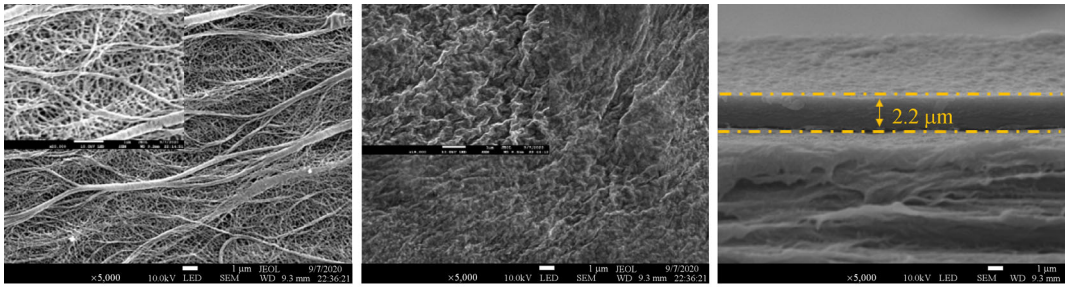

Fig. 4 (a) The surface image of the PE microfiltration membrane; (b) CMC-Na/GA-PE composite membrane (CMC-Na:GA = 6:4, crosslinked in 4 h); (c) the cross-section image of the composite membrane.

membranes are given in Fig. 5. According to Fig. 5(a), as the mass ratio of CMC-Na:GA increases from 6:3 to 6:8, the membrane flux gradually decreases from 38.47 to 27.46 $kg \cdot m^{-2} \cdot h^{-1}$ while the salt rejection increases from 99.76% to 99.99%. This is due to that at a higher crosslinker concentration, a highly crosslinked CMC-Na/GA structure is obtained. This result is consistent with the decrements in the swelling degrees of the crosslinked polymers. As shown in Fig. 5(c), the polymer's swelling degree gradually decreases from 33% to 15%. This corresponds to a monotonically decreased value of $\overline{M_c}$ as shown in Fig. 5(d). To obtain a composite membrane with both a high flux and a high salt rejection, a CMC-Na:GA mass ratio of 6:4 is chosen. At this composition, as the crosslinking time increases from 2 to 5 h, the salt rejection increases but the membrane flux decreases as shown in Fig. 5(b). Since the salt rejection is barely increased when the crosslinking time is higher than 4 h, 4 h is selected as the crosslinking time. In summary, the optimized fabrication condition of the composite membranes is determined where a 2 wt-% CMC-Na/GA coating solution with a CMC-Na:GA mass ratio of 6:4 is selected at the coating solution and the crosslinking time.

3.4 The alkali resistance of the composite membrane

To evaluate the alkali resistance, a composite membrane was soaked in a 20 wt-% NaOH for 9 d at 25 °C, where the flux and rejection were measured every three days as shown in Fig. S1 (cf. Electronic Supplementary Material, ESM). No observable changes in membrane flux and salt rejection is observed. Figure S1(b) shows that the chemical structure of the CMC-Na/GA layer is unchanged after the alkali treatment [22,43]. There are no observable changes in color and surface topography of the membranes after soaking in the alkaline solution. Similarly, the EDS spectra in Fig. S1(c) indicate that the atomic concentrations of C and O are not changed but that of Na increases. This is because the remaining COOH groups in CMC-Na react with NaOH to produce sodium carboxylate. Not that, the formation of sodium carboxylate does not affect the crosslinking structure.

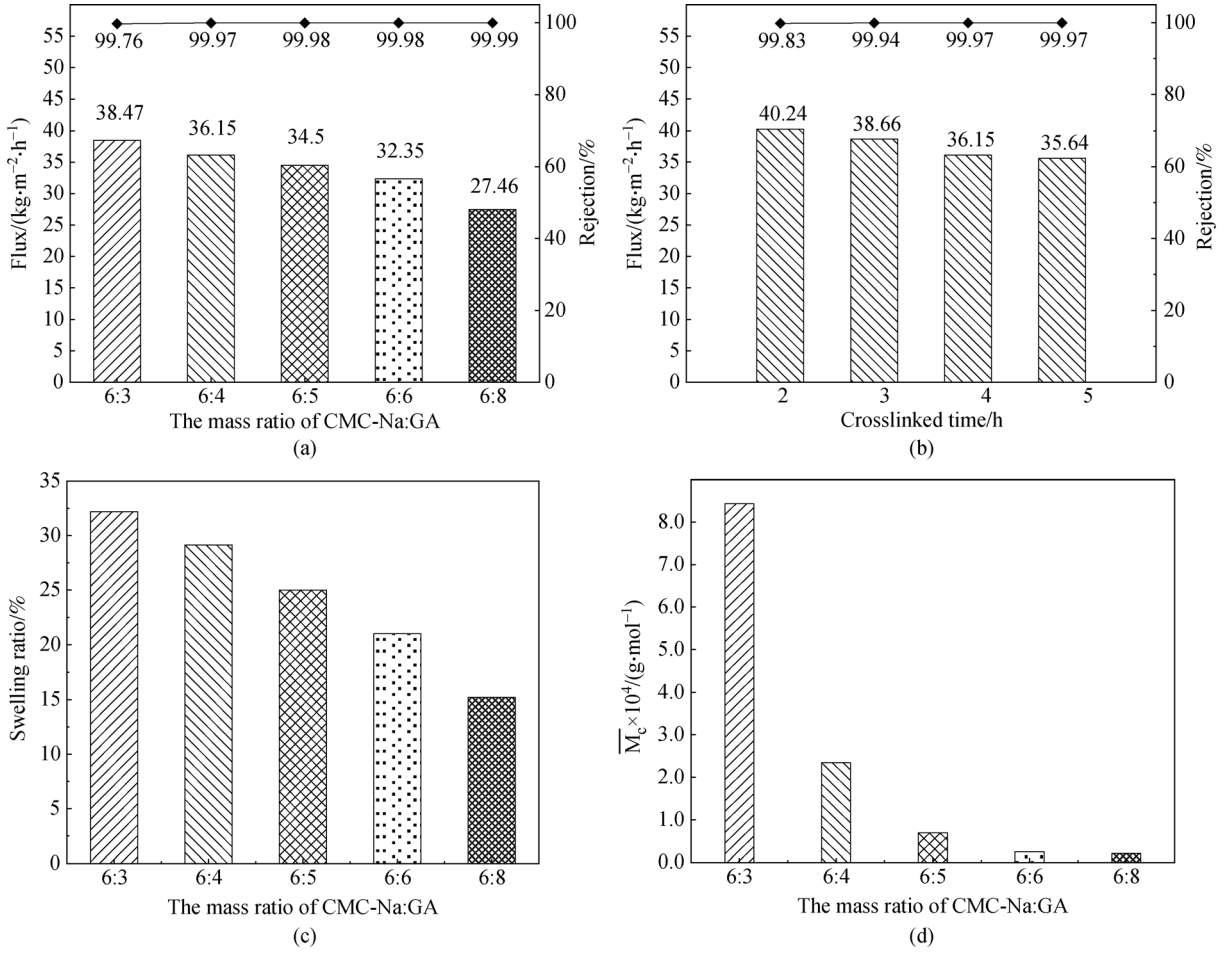

Fig. 5 The pervaporation desalination performance at 70 °C for composite membranes prepared using (a) different CMC-Na:GA solutions, (b) different crosslinked times; the effects of GA concentrations on (c) the swelling ratios and (d) $\overline{M_c}$ of the GA crosslinked CMC-Na polymers.

Since pervaporation test is typically carried out at relatively high temperatures, the alkali resistance of the composite membrane is further evaluated at 60 °C. As shown in Fig. 6, the salt rejection of the composite membrane is maintained at 99.5% and the normalized membrane fluxes are fluctuated at 32 ± 4 kg·m^{-2}·h^{-1} during an 80 h soaking period in a 10 wt-% NaOH aqueous solution at 60 °C. Moreover, the FTIR spectra of the composite membrane show no observable changes as shown in Figs. 6(c) and 6(d). This is another proof for the excellent alkali resistance. Figure 6(b) shows the water contact angles of the pristine PE membrane, and the CMC-Na/GA-PE composite membrane before and after the alkali treatment. Water contact angles of the pristine PE and composite membranes are 99° and 54.85°, respectively. After being soaked in the alkaline solution, the water contact angle of the composite membrane is 56.9°. Therefore, there was no significantly change in surface hydrophilicity. In summary, the results of pervaporation desalination tests, FTIR spectra, and surface hydrophilicity prove that the composite membrane is stable in high temperature alkaline solution.

3.5 The thermal stability CMC-Na/GA self-supporting membrane

The TGA curves of the CMC-Na/GA self-supported membrane before and after 15 d of NaOH immersing at 25 °C are provided in Fig. 7. The first weight loss in a temperature range of 50 °C–150 °C is due to the water evaporation. The second weight loss happens in 268 °C–334 °C, where the carboxyl groups decompose. The last weight loss takes place in 340 °C–500 °C. This indicates the degradation of the main polymer chains of the CMC-Na. It shows that after the alkali treatment, thermal decomposition in the temperature range of 268 °C–334 °C is more significant. It is because the reaction between NaOH and the –COOH groups breaks down the hydrogen bonding. Thus, the thermal stability decreases. In the following decomposition stage of 340 °C–500 °C, the

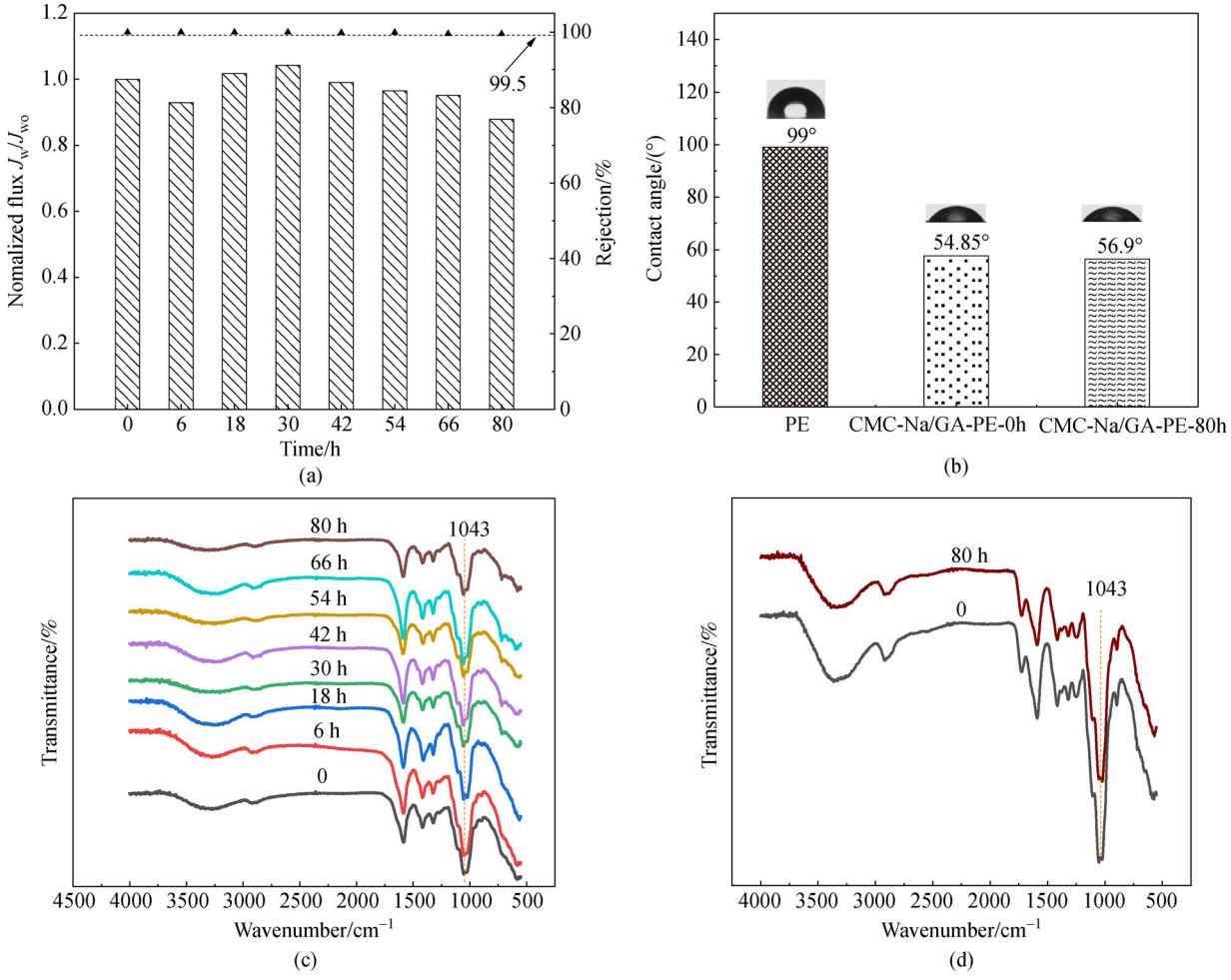

Fig. 6 (a) The normalized fluxes of the pervaporation composite membrane after being soaked in alkaline solutions; (b) the water contact angles of the membranes; (c) and (d) the FTIR spectra of the membranes after immersed in 10 wt-% NaOH for different times.

alkali treated membrane shows lower decomposition rate. This is because the existence of Na^+ cation in the polymer increases the residual mass.

3.6 The mechanical property of CMC-Na/GA self-supporting membrane

The mechanical properties of the GA crosslinked films before and after the alkali treatment were determined using a DMA equipment. As shown in Fig. S2 (cf. ESM), the fracture strain of the film increases from 0.5% to 0.97%, while the tensile strength decreases from 12.33 to 7.27 MPa after it is soaked in 20 wt-% NaOH solution for 15 d at 25 °C. This is mainly attributed to that intermolecular hydrogen bonds were broken after the alkali treatment. It could lead to the decrement in the crystallizing domains and decrease the mechanical strength. To further explore the change of the crystalline and amorphous structures before and after the NaOH treatment, we analyzed the films by XRD. As shown in Fig. S3 (cf. ESM), the percentage of crystallization domain is 56.24%, while it decreases to 33% after the NaOH-soaking.

3.7 Evaluation of the dynamic alkali-resistance of the composite membranes

The dynamic alkali-resistance of the composite membranes and the concentrating NaOH solution were shown in Fig. 8. A 36 h alkali-resistance test of the composite membrane is carried out for treating a 10 wt-% NaOH solution at 60 °C. As shown in Fig. 8(a), the composite membrane shows a relatively stable water flux and high NaOH rejection of 99.98% during the entire experiment period. The slightly decrement in water flux over time is caused by the scaling of NaOH on the membrane surface. After the dynamic alkali pervaporation test, the membrane is further tested for desalination performance and a high salt rejection of 99.98% is obtained. Figure 8(b) shows the pervaporation experiment for concentrating a NaOH solution from 5 to 10 wt-%. It can be seen that the

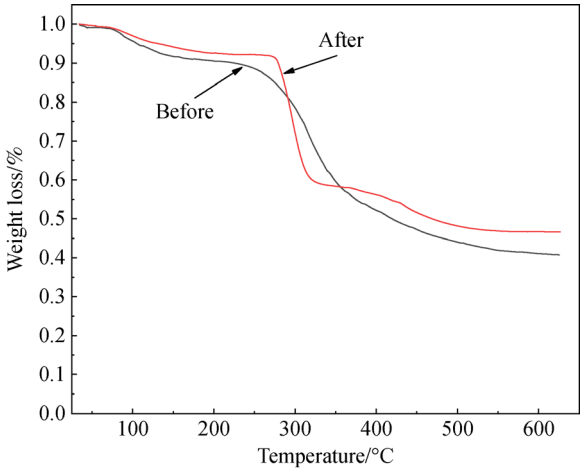

Fig. 7 The TGA of CMC-Na/GA self-supporting membrane before and after 15 d of NaOH immersing at 25 °C.

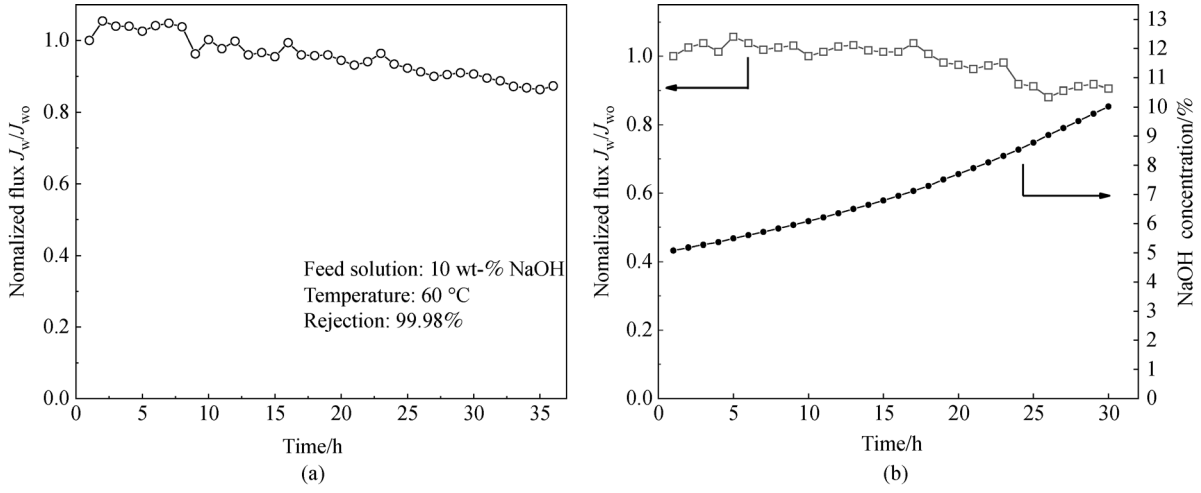

Fig. 8 (a) The normalized flux change for the dynamic alkali resistance pervaporation test (the feed solution is 10 wt-% NaOH and the temperature is 60 °C); (b) the normalized flux change during a NaOH enrichment test (from 5 to 10 wt-%).

NaOH rejection is 99.98% and the water flux gradually decreases due to increase in the NaOH concentration of the feed solution. Table 1 compares the separation performances of some representative membranes with the CMC-Na/GA-PE membranes. No membranes have been tested at a NaOH concentation over 10 wt-% except for our membranes. All the above results demonstrate the excellent alkali resistance of the composite membrane and its potential for concentrating alkali solutions.

3.8 Acid resistance and chlorine resistance of the composite membrane

Figure 9 shows that the salt rejection and water flux of the composite membrane does not change after it is soaked in a 4 wt-% H_2SO_4 at 25 °C for 9 d. Besides, it shows that the desalination property of the composite membrane is not affect by soaking in a 500 mg·L^{-1} chlorine solution for 9 d. Therefore, the membrane is stable in acid and chlorine solutions.

3.9 Evaluation of the fouling resistance of the composite membrane

Membrane fouling is a serious problem in water treatment [50]. To evaluate the pollution resistance of the CMC-Na/GA-PE composite membranes, 5000 mg·L^{-1} HA and SA are chosen as organic [51] and biofouling [50] pollutants. As shown in Fig. 10, the two membranes show stable water fluxes of 38 ± 2 kg·m^{-2}·h^{-1}. In the first two hours of HA rejection experiment, the water flux drops to 94.6%. In the rest of the experiment, the water fluxes are stable, which may be due to the dynamic equilibrium achieved by HA in adsorption-desorption on the membrane surface. In the 24 h SA rejection test, the water flux drops to 93.8% in the first 2 h and becomes stable. Similarly, the initial drop is due to the quick adsorption of SA on the membrane surface. Note that, the overall flux drops are very limited. This is due to the hydrophilic nature of the CMC-Na dense layer that exhibits a high resistance to organic and biofouling.

Table 1 Separation properties of alkali-resistant membranes [a)]

Membrane type	Material	NaOH concentration/%	Alkali test method	Membrane flux/(L·m^{-2}·h^{-1}·bar^{-1})	Rejection/%
RO [44]	PA	0.04	Immersing	5.28	99.06
NF [45]	PVA-CMC-Na	1.96	Immersing	17.96	38.2
NF[46]	PVA-APES	4.0	Immersing	13.5	53.6
UF [47]	Polyphenylsulfone	0.38	Immersing	0.675	–
MF [48]	PPS	3.85	Immersing	154.95	–
Pervaporation [49]	PVA-FS/PVDF	0.38	Immersing	34 [b)]	99.9
Pervaporation (This study)	CMC-Na/GA-PE	20	Immersing (25 °C)	35 [b)]	99.9 ± 0.1
Pervaporation (This study)	CMC-Na/GA-PE	10	Circulation (60 °C)		

a) RO: reverse osmosis; NF: nanofiltration; UF: ultrafiltration; MF: microfiltration; PVA: poly(vinyl alcohol); PA: Polyamide; APES: aminopropyl triethoxysilane; PPS: poly(p-phenylene sulfide); FS: a fluorocarbon surfactant; PVDF: poly (vinylidene fluoride). b) The unit of membrane flux: L·m^{-2}·h^{-1}.

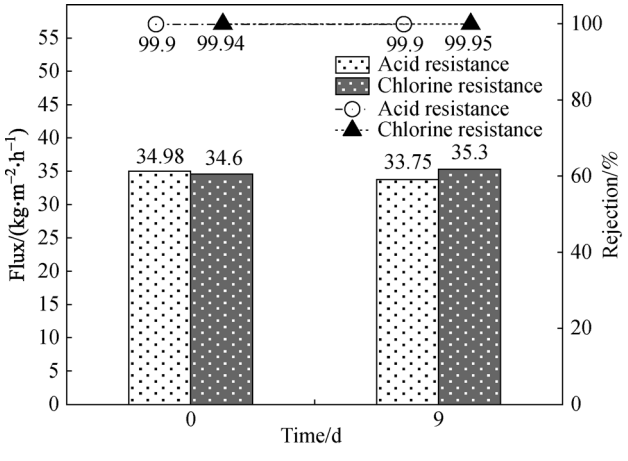

Fig. 9 The static acid and chlorine resistance tests of composite membranes at 25 °C (the temperature of 3.5% NaCl feed solution was 70 °C, and the pressure of permeate side was 100 Pa).

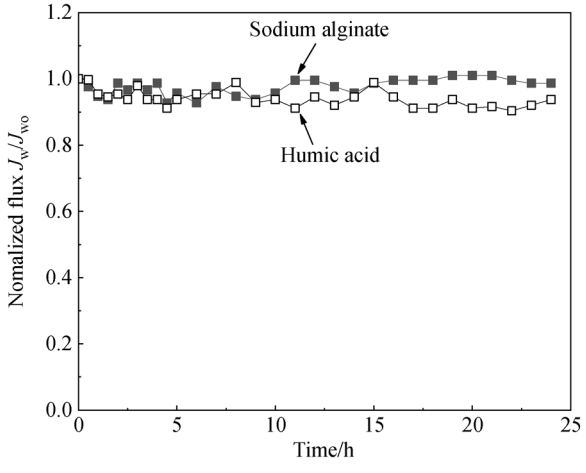

Fig. 10 The normalized membrane fluxes of the long-time test using the water solutions containing 5000 mg·L^{-1} HA or SA.

4 Conclusions

In this paper, we prepared a series of CMC-Na/GA-PE composite pervaporation membrane by spray-coating and post crosslinking. By optimizing the membrane fabrication conditions, the composite membrane possesses a flux of 35 ± 2 $kg \cdot m^{-2} \cdot h^{-1}$ and a salt rejection of 99.9% for separating a 3.5 wt-% NaCl solution at 70 °C and an average water flux of 23 $kg \cdot m^{-2} \cdot h^{-1}$ with a NaOH rejection over 99.98% when concentrating a NaOH solution from 5 to 10 wt-% at 60 °C. The pervaporation composite membranes are stable in a 20 wt-% NaOH solution that is 5-fold as high as the highest concentration being attempted in other membranes. Thus, the CMC-Na/GA-PE pervaporation composite membrane has a great potential for concentrating alkali solutions and is suitable for applied in harsh environments.

Acknowledgements This research is funded by the National Natural Science Foundation of China (Grant No. 51773011).

Electronic Supplementary Material Supplementary material is available in the online version of this article at https://dx.doi.org/10.1007/s11705-021-2078-2 and is accessible for authorized users.

References

1. Mathew M L, Gopalakrishnan A, Aravindakumar C T, Aravind U K. Low-cost multilayered green fiber for the treatment of textile industry waste water. Journal of Hazardous Materials, 2019, 365: 297–305
2. Buscio V, López Grimau V, Álvarez M D, Gutiérrez Bouzán C. Reducing the environmental impact of textile industry by reusing residual salts and water: ECUVal system. Chemical Engineering Journal, 2019, 373: 161–170
3. Jia C, Chen C, Kuang Y, Fu K, Wang Y, Yao Y, Kronthal S, Hitz E, Song J, Xu F, et al. From wood to textiles: top-down assembly of aligned cellulose nanofibers. Advanced Materials, 2018, 30(30): 1801347
4. Mirmohamadsadeghi S, Karimi K, Azarbaijani R, Parsa Yeganeh L, Angelidaki I, Nizami A S, Bhat R, Dashora K, Vijay V K, Aghbashlo M, et al. Pretreatment of lignocelluloses for enhanced biogas production: a review on influencing mechanisms and the importance of microbial diversity. Renewable & Sustainable Energy Reviews, 2021, 135: 110173
5. Al Amshawee S, Yunus M Y B M, Azoddein A A M, Hassell D G, Dakhil I H, Hasan H A. Electrodialysis desalination for water and wastewater: a review. Chemical Engineering Journal, 2020, 380: 122231
6. Hao J, Wu Y, Ran J, Wu B, Xu T. A simple and green preparation of PV A-based cation exchange hybrid membranes for alkali recovery. Journal of Membrane Science, 2013, 433: 10–16
7. Padaki M, Surya Murali R, Abdullah M S, Misdan N, Moslehyani A, Kassim M A, Hilal N, Ismail A F. Membrane technology enhancement in oil-water separation: a review. Desalination, 2015, 357: 197–207
8. He S, Jiang X, Li S, Ran F, Long J, Shao L. Intermediate thermal manipulation of polymers of intrinsic microporous (PIMs) membranes for gas separations. AIChE Journal. American Institute of Chemical Engineers, 2020, 66(10): 16543
9. Yang F, Sadam H, Zhang Y, Xia J, Yang X, Long J, Songwei L, Shao L. A *de novo* sacrificial-MOF strategy to construct enhanced-flux nanofiltration membranes for efficient dye removal. Chemical Engineering Science, 2020, 225: 115845
10. Zhang Y, Cheng X, Jiang X, Urban J J, Lau C H, Liu S, Shao L. Robust natural nanocomposites realizing unprecedented ultrafast precise molecular separations. Materials Today, 2020, 36: 40–47
11. Wang J J, Yang H C, Wu M B, Zhang X, Xu Z K. Nanofiltration membranes with cellulose nanocrystals as an interlayer for unprecedented performance. Journal of Materials Chemistry. A, Materials for Energy and Sustainability, 2017, 5(31): 16289–16295
12. Verbeke R, Gómez V, Vankelecom I F J. Chlorine-resistance of reverse osmosis (RO) polyamide membranes. Progress in Polymer Science, 2017, 72: 1–15
13. Xu Y M, Japip S, Chung T S. UiO-66-NH_2 incorporated dual-layer hollow fibers made by immiscibility induced phase separation (I2PS) process for ethanol dehydration via pervaporation. Journal of Membrane Science, 2020, 595: 117571
14. Liang B, Li Q, Cao B, Li P. Water permeance, permeability and desalination properties of the sulfonic acid functionalized composite pervaporation membranes. Desalination, 2018, 433: 132–140
15. Xue Y, Lau C H, Cao B, Li P. Elucidating the impact of polymer crosslinking and fixed carrier on enhanced water transport during desalination using pervaporation membranes. Journal of Membrane Science, 2019, 575: 135–146
16. Zhang R, Xu X, Cao B, Li P. Fabrication of high-performance PVA/PAN composite pervaporation membranes crosslinked by PMDA for wastewater desalination. Petroleum Science, 2018, 15(1): 146–156
17. Li Q, Cao B, Li P. Fabrication of high performance pervaporation desalination composite membranes by optimizing the support layer structures. Industrial & Engineering Chemistry Research, 2018, 57 (32): 11178–11185
18. Meng J, Li P, Cao B. High-flux direct-contact pervaporation membranes for desalination. ACS Applied Materials & Interfaces, 2019, 11(31): 28461–28468
19. Haleem N, Arshad M, Shahid M, Tahir M A. Synthesis of carboxymethyl cellulose from waste of cotton ginning industry. Carbohydrate Polymers, 2014, 113: 249–255
20. Lakshmi D S, Trivedi N, Reddy C R K. Synthesis and characterization of seaweed cellulose derived carboxymethyl cellulose. Carbohydrate Polymers, 2017, 157: 1604–1610
21. Prasad C V, Sudhakar H, Swamy B Y, Reddy G V, Reddy C L N, Suryanarayana C, Prabhakar M N, Subha M C S, Rao K C. Miscibility studies of sodium carboxymethylcellulose/poly(vinyl alcohol) blend membranes for pervaporation dehydration of isopropyl alcohol. Journal of Applied Polymer Science, 2011, 120 (4): 2271–2281
22. Zhang Y H, Yu C, Lu Z H, Yu S C. Modification of polysulfone ultrafiltration membrane by sequential deposition of cross-linked poly(vinyl alcohol) (PVA) and sodium carboxymethyl cellulose (CMCNa) for nanofiltration. Desalination and Water Treatment,

2016, 57(38): 17658–17669
23. Gao F S. Study on novel negative charged composite nanofiltration membrane from chitin/CMC macromolecule. Dissertation for the Master Degree. Qingdao: Ocean University of China, 2007, 1–74
24. Zheng Z R, Gu Z Y, Huo R T, Luo Z S. Superhydrophobic poly (vinylidene fluoride) film fabricated by alkali treatment enhancing chemical bath deposition. Applied Surface Science, 2010, 256(7): 2061–2065
25. Ross G J, Watts J F, Hill M P, Morrissey P. Surface modification of poly(vinylidene fluoride) by alkaline treatment. Part 2. Process modification by the use of phase transfer catalysts. Polymer, 2001, 42(2): 403–413
26. Yin Q, Zhang Q, Cui Z L, Li W X, Xing W H. Alkali resisting polyphenylsulfone ultrafiltration membrane with tailored microstructure. Polymer, 2017, 124: 128–138
27. Zuo J, Bonyadi S, Chung T. Exploring the potential of commercial polyethylene membranes for desalination by membrane distillation. Journal of Membrane Science, 2016, 497: 239–247
28. Li J M, Xu Z K, Liu Z M, Yuan W F, Xiang H, Wang S Y, Xu Y Y. Microporous polypropylene and polyethylene hollow fiber membranes. Part 3. Experimental studies on membrane distillation for desalination. Desalination, 2003, 155(2): 153–156
29. Zuo J, Bonyadi S, Chung T S. Exploring the potential of commercial polyethylene membranes for desalination by membrane distillation. Journal of Membrane Science, 2016, 497: 239–247
30. Park S H, Kwon S J, Shin M G, Park M S, Lee J S, Park C H, Park H, Lee J H. Polyethylene-supported high performance reverse osmosis membranes with enhanced mechanical and chemical durability. Desalination, 2018, 436: 28–38
31. Kwon S J, Park S H, Park M S, Lee J S, Lee J. Highly permeable and mechanically durable forward osmosis membranes prepared using polyethylene lithium ion battery separators. Journal of Membrane Science, 2017, 544: 213–220
32. Kwon S J, Park S H, Shin M G, Park M S, Park K, Hong S, Park H, Park Y I, Lee J. Fabrication of high performance and durable forward osmosis membranes using mussel-inspired polydopamine-modified polyethylene supports. Journal of Membrane Science, 2019, 584: 89–99
33. Li M S, Zhao Z P, Wang M X. Green hydrophilic modification of PE hollow fiber membranes in a module scale via long-distance and dynamic low-temperature H_2O plasma flow. Applied Surface Science, 2016, 386: 187–195
34. Sheng L, Song L, Gong H, Pan J, Bai Y, Song S, Liu G, Wang T, Huang X, He J. Polyethylene separator grafting with polar monomer for enhancing the lithium-ion transport property. Journal of Power Sources, 2020, 479: 228812
35. Belmonte G K, Charles G, Strumia M C, Weibel D E. Permanent hydrophilic modification of polypropylene and poly(vinyl alcohol) films by vacuum ultraviolet radiation. Applied Surface Science, 2016, 382: 93–100
36. Meng J, Lau C H, Xue Y, Zhang R, Cao B, Li P. Compatibilizing hydrophilic and hydrophobic polymers via spray coating for desalination. Journal of Materials Chemistry. A, Materials for Energy and Sustainability, 2020, 8(17): 8462–8468
37. Yun Long X, Huang J, Lau C, Cao B, Li P. Tailoring the molecular structure of crosslinked polymers for pervaporation desalination. Nature Communications, 2020, 11(1): 1461
38. Vetere A. Empirical method to correlate and to predict the vapor-liquid equilibrium and liquid-liquid equilibrium of binary amorpous polymer solutions. Industrial & Engineering Chemistry Research, 1998, 37(7): 2864–2872
39. Amiri A, Triplett Z, Moreira A, Brezinka N, Alcock M, Ulven C A. Standard density measurement method development for flax fiber. Industrial Crops and Products, 2017, 96: 196–202
40. Mulder M H V, Smolders C A. On the mechanism of separation of ethanol/water mixtures by pervaporation I. Calculations of concentration profiles. Journal of Membrane Science, 1984, 17(3): 289–307
41. Yu S, Zhang X, Tan G, Tian L, Liu D, Liu Y, Yang X, Pan W. A novel pH-induced thermosensitive hydrogel composed of carboxymethyl chitosan and poloxamer cross-linked by glutaraldehyde for ophthalmic drug delivery. Carbohydrate Polymers, 2017, 155: 208–217
42. Das B, Ray D, De R. Influence of sodium carboxymethylcellulose on the aggregation behavior of aqueous 1-hexadecyl-3-methylimidazolium chloride solutions. Carbohydrate Polymers, 2014, 113: 208–216
43. Shao L L, An Q F, Ji Y L, Zhao Q, Wang X S, Zhu B K, Gao C J. Preparation and characterization of sulfated carboxymethyl cellulose nanofiltration membranes with improved water permeability. Desalination, 2014, 338: 74–83
44. Liu Y, Yan W, Wang Z, Wang H, Zhao S, Wang J, Zhang P, Cao X. 1-Methylimidazole as a novel additive for reverse osmosis membrane with high flux-rejection combinations and good stability. Journal of Membrane Science, 2020, 599: 117830
45. Zhang Y, Yu C, Lu Z, Yu S. Modification of polysulfone ultrafiltration membrane by sequential deposition of cross-linked poly(vinyl alcohol) (PVA) and sodium carboxymethyl cellulose (CMCNa) for nanofiltration. Desalination and Water Treatment, 2016, 57(38): 17658–17669
46. Zhang Y, Guo M, Yan H, Pan G, Xu J, Shi Y, Liu Y. Novel organic-norganic hybrid composite membranes for nanofiltration of acid and alkaline media. RSC Advances, 2014, 4(101): 57522–57528
47. Yin Q, Zhang Q, Cui Z, Li W, Xing W. Alkali resisting polyphenylsulfone ultrafiltration membrane with tailored microstructure. Polymer, 2017, 124: 128–138
48. Gao Y, Li Z, Cheng B, Su K. Superhydrophilic poly(*p*-phenylene sulfide) membrane preparation with acid/alkali solution resistance and its usage in oil/water separation. Separation and Purification Technology, 2018, 192: 262–270
49. Zhao P, Xue Y, Zhang R, Cao B, Li P. Fabrication of pervaporation desalination membranes with excellent chemical resistance for chemical washing. Journal of Membrane Science, 2020, 611: 118367
50. Charfi A, Jang H, Kim J. Membrane fouling by sodium alginate in high salinity conditions to simulate biofouling during seawater desalination. Bioresource Technology, 2017, 240: 106–114
51. Naidu G, Jeong S, Kim S J, Kim I S, Vigneswaran S. Organic fouling behavior in direct contact membrane distillation. Desalination, 2014, 347: 230–239